ON MODELING THE POST BREAKING PHASE: SPLASHING

E. Fontaine, M. Landrini and M.P. Tulin

Ocean Engineering Laboratory, UCSB, CA93106-1080, USA

Wave breaking is known to play a crucial role in explaining various phenomena such as the down-shifting evolution of ocean wind waves [1], high impact loads on structures [2], the observed high RCS return at low grazing angles [3], or the existence of a visible surface wake behind ships [4]. In the latter case, part of the persisting surface disturbance is the result of bow wave breaking, and it is desiderable to understand and quantify this process. As a wave breaks, several regimes have been identified, [5], [6]:

- Steepening-cresting phase. The wave is deforming asymmetrically, its crest and trough rise, the front face steepens: and the crest eventually sharpens.
- Plunging-jet phase. A jet forms at the crest of the deformed wave and moves forward and downward in a ballistic trajectory.
- Splashing-ploughing phase. The plunging jet has splashed into the front face of the wave, throwing water upwards as it ploughs forward. Air entrainment usually occurs during this phase.
- Decaying scar phase. The turbulent underwater structure created during the previous phase is slowly dissipated under the action of viscosity.

The steepening-cresting and plunging-jet phases can be accurately simulated within the framework of potential flow theory, and using Boundary Element Method (BEM) in a Mixed Eulerian Lagrangian (MEL) approach. Simulation of energetic ocean breaking waves have been carried out successfully up to the early beginning of the splashing-ploughing phase, i.e. as the tip of the jet starts to re-enters the front face of the wave, [5], [6]. Similarly, bow breaking waves have been simulated within the framework of $2D + t$ theory, [7], [8]. Despite attempts to directly simulate the overall breaking process [9], little is known about the detailed mechanisms that lead to air entrapment and to the formation of the resulting post-breaking vortical structures which give rise to the visible wake.

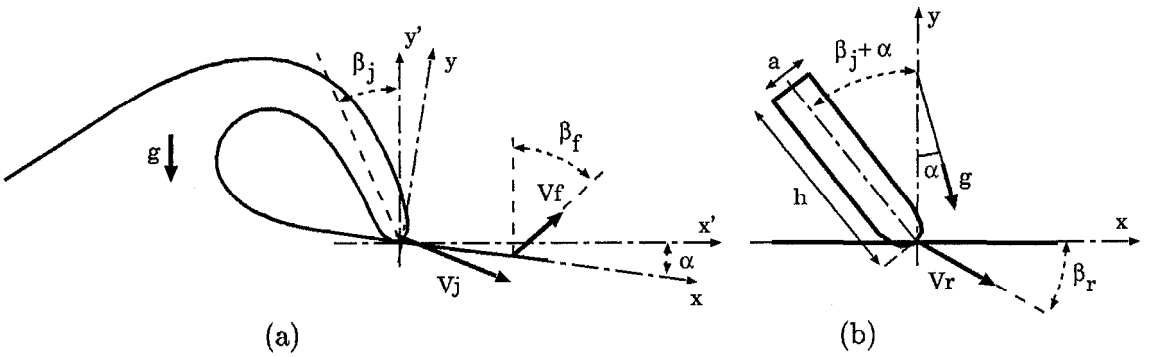

Figure 1: (a) Breaking wave at the beginning of the splashing-ploughing phase, and (b) the associated simplified model with gravity and neglecting surface tension.

The aim of the present study is to extend our knowledge of the splashing-ploughing phase through the simplified modeling presented in Fig. 1, preparatory to calculating the complete

problem, (a), using a hybrid method. The jet is here represented by a two-dimensional slug of water in free-fall which hits the surface (front face of the wave) at some angle from the vertical. In a frame of reference moving upwards with the front face, the gravity and relative velocity of the jet appear to be tilted with respect to the vertical and the jet axis directions, respectively. The main parameters in the problem are the aspect ratio of the jet, $r = h/a$, the Froude number $F = V_r/\sqrt{ga}$, and the angles α, β_j and β_r.

The simplified problem, (b), can be studied within the framework of potential flow theory and using BEM [10], but this approach is limited both by necessary theoretical assumptions and technical difficulties associated with following highly distorted free-surface configurations. In particular, fluid fragmentation is observed during the splashing phase.

Here, the Smoothed Particle Hydrodynamics (SPH) method [11] was adopted. This fully Lagrangian method was initially designed for the resolution of compressible Euler equations with applications to astrophysical problems [12]. The key concept of the method is to give a local approximation of a generic physical variable $f(\vec{x}, t)$ in terms of the values f_i (t) carried by a finite number of particles, i.e.

$$f(\vec{x},t) = \iint f(\vec{x'},t)\,\delta(\vec{x}-\vec{x'})\,ds \simeq \iint f(\vec{x'},t)\,W(\vec{x}-\vec{x'})\,ds \simeq \Sigma_j \frac{m_j}{\rho_j} f(\vec{x_j},t)\,W(\|\vec{x}_j-\vec{x}\|) \quad (1)$$

where the smoothing kernel $W(\vec{x})$ is an approximation to the Dirac δ function, m_i and ρ_i are the mass and density of the fluid particle. Upon identifying f with the variables ρ and $\vec{U}$, Euler equations reduce to a set of ODEs that are integrated with respect to time to give the evolution of the fluid dynamic system. Spatial derivatives of the quantities are obtained by differentiating eq. (1), i.e. using analytical kernel derivatives. The compact support of the kernel leads each particle to interact only with its close neighbours. Mass and momentum conservation are explicitely enforced by requiring each particle to have a constant mass and symmetric interactions between them, respectively. The pressure is computed by using the density and a suitable equation of state for water which is considered a weakly compressible fluid. Simulations are performed at a low Mach number (typically $M = 0.1$), leading to non essential perturbations in density during the simulation (typically of the order of $O(M^2) = 0.01$). As in most numerical methods, artificial viscosity is introduced to stabilize the scheme. Changes in the total energy, typically within a few percent, are representative of the global accuracy of the simulations. The method has been implemented and successfully tested against both analytical and BEM results for different problems: the evolution of a patch of fluid, the propagation of a bore, the wedge entry problem, and the generation and propagation of shallow water waves. Results will be presented.

A particular SPH simulation of the prototype problem, (b), is shown in Fig. 2, where the parameters are based on the LONGTANK simulation of an energetic breaker [5], using 100^K particles distributed in the water with variable initial spacings, densest near the surface. Hydrostatic pressure is imposed on the outer boundary of the flow domain (not shown).

The jet does not decelerate significantly after impact, and the impacting fluid is deflected upwards on the left covering the previous surface; and similarly on the right, where it spills over together with some of the former surface, forming a visible splash up. After some time, the observed shape of the impacting jet and the new surface tend to become unchanging, see Fig. 2 lower right corner, and the particles on the upper side of the new cavity surface are almost motionless. The very thin jet formed on the right is seen to be stretching, fragmenting and falling downwards. The observed behaviour has important implications for the generation of vorticity.

Simulations have also been conducted for a range of jet parameters with interesting results. For $F > O(10)$ and $\beta < O(20°)$, Fig. 3, the impacting jet flow into the cavity on the left tends to disappear and the slug is deflected along the surface; ricochet is indicated. For $F <$ O(3) the cavity eventually collapses creating an upward splash (see Fig. 4).

Finally, a hybrid numerical procedure is under development where the the splashing jet region, modeled by SPH numerics, is driven by the surrounding wave field described by BEM

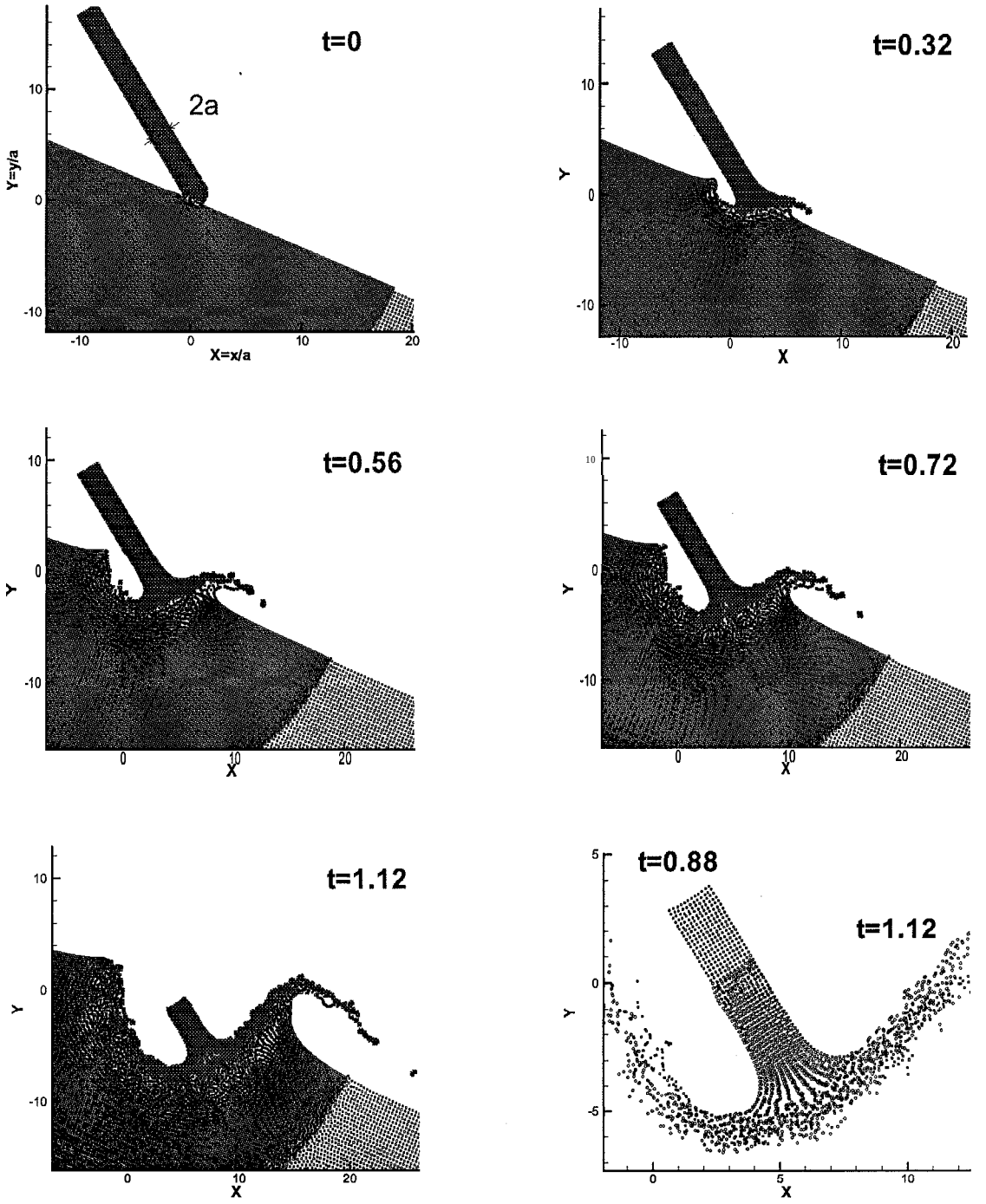

Figure 2: Jet breaking wave at the beginning of the splashing-ploughing phase for a = 23°, β_j = 31°, β_r = 30°, F = 10, and r = 10.

numerics. Coupling is achieved by partial overlapping of the two subdomains. The SPH method allows the eventual inclusion of multiphase effects due to air entrapment.

The authors are grateful for the support of the ONR, Dr Ed Rood, Program Manager.

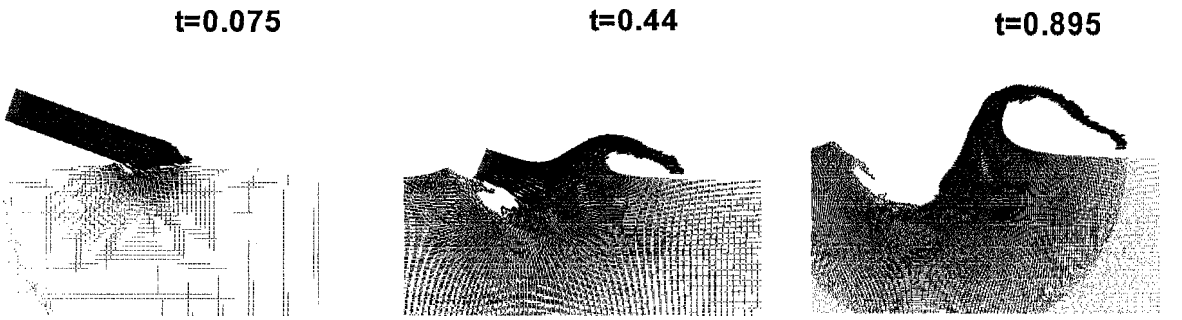

Figure 3: Jet breaking wave at the beginning of the splashing-ploughing phase for α = 0°, $\beta_j = 70°$, $\beta_r = 20°$, $F = 10$, and r = 10. The scales differs in each plot.

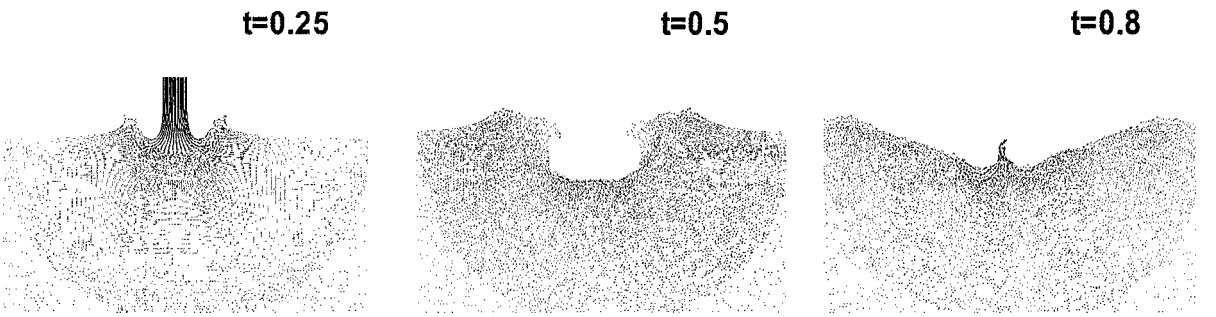

Figure 4: Jet breaking wave at the beginning of the splashing-ploughing phase for α = 0°, $\beta_j = 0°$, $\beta_r = 90°$, $F = 1$, and r = 10. BEM simulation stops [10] after t=0.5 as the cavity collapses.

References

[1] M.P. Tulin, Y. Yao, A.K. Magnusson, 1996. The evolution and structure of energetic wind waves, *Proc. of ISOPE'96.*

[2] S. Welch, C. Levi, E. Fontaine, M.P. Tulin, 1999. Experimental loads on a flexibly mounted vertical cylinder in breaking waves groups. **International Journal on** Offshore and Polar Engineering (in Press).

[3] J. Fuchs, D. Regas, T. Waseda, S. Welch and M.P. Tulin, 1999. Correlation of hydrodynamics features with LGA Radar Backscatter fron breaking waves. *IEEE* transactions *on Geoscience and remote* sensing, Vol. 37, No 5, pp. 2442-2460.

[4] I. Miyata and T. Inui, 1984. Nonlinear ship waves, Advances in *Applied* Mechanics, Vol. 24, pp. 215-289.

[5] M.P. Tulin, Y. Yao, and P. Wang, 1994. The simulation of the deformation and breaking of ocean waves in wave groups. *BOSS'94*, Boston-Ma, pp. 383-392.

[6] M.P. Tulin and T. Waseda, 1999. Laboratory observations of wave group evolution, including breaking effects. *J.* Fluid *Mech.*, vol. 378, pp. 197-232.

[7] M.P. Tulin and T. Wu, 1996. Divergent Bow Waves. In *Twenty* **first** Symposium on Naval Hydrodynamics, *Trondheim,* Norway, *pp. 99-117.*

[8] E. Fontaine and M.P. Tulin, 1998. On the prediction of nonlinear free-surface flows past slender hulls using $2D + t$ approximation: the evolution of an idea. *Proc.* Symp. *NATO/RTO/AVT*, pp. 26-1,11, Amsterdam.

[9] I. Miyata, 1995. Potential flow of fluids, CMP, Ed. M. Rahman.

[10] A. Prosperetti and H. N. Oguz, 1997. Air entrainment upon liquid impact. *Phil. Trans. R. Soc.* Lond. A, Vol. 355, pp. 491-506.

[11] J.J Monaghan and A. Kos, 1999. Solitary Waves on a Cretan Beach. Journal of Waterway, *Port, and* Ocean Engineering, May/June, pp. 145-154.

[12] J.J. Monaghan, 1992. Smoothed Particle Hydrodynamics. *Annu. Rev.* Astron. *Astrophys., 30,* pp. 543-574.